

Particle-Based Porous Materials for the Rapid and Spontaneous Diffusion of Liquid Metals

Jian Shu, Yangming Lu, Erlong Wang, Xiangpeng Li,* Shi-Yang Tang,* Sizepeng Zhao, Xiangbo Zhou, Lining Sun, Weihua Li, and Shiwu Zhang*



Cite This: *ACS Appl. Mater. Interfaces* 2020, 12, 11163–11170



Read Online

ACCESS |



Metrics & More



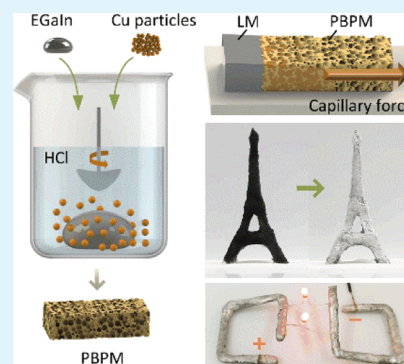
Article Recommendations



Supporting Information

ABSTRACT: Gallium-based room-temperature liquid metals have enormous potential for realizing various applications in electronic devices, heat flow management, and soft actuators. Filling narrow spaces with a liquid metal is of great importance in rapid prototyping and circuit printing. However, it is relatively difficult to stretch or spread liquid metals into desired patterns because of their large surface tension. Here, we propose a method to fabricate a particle-based porous material which can enable the rapid and spontaneous diffusion of liquid metals within the material under a capillary force. Remarkably, such a method can allow liquid metal to diffuse along complex structures and even overcome the effect of gravity despite their large densities. We further demonstrate that the developed method can be utilized for prototyping complex three-dimensional (3D) structures via direct casting and connecting individual parts or by 3D printing. As such, we believe that the presented technique holds great promise for the development of additive manufacturing, rapid prototyping, and soft electronics using liquid metals.

KEYWORDS: liquid metal, diffusion, porous materials, capillary force, rapid prototyping



INTRODUCTION

From nature where trees transport water and nutrients from the soil based on the capillary effect to oil rising along the wick to light up the darkness, the capillary effect is ubiquitous in our daily life and in industrial and agricultural areas.^{1–3} After hundreds of years of research, the capillary effect has been applied in various areas such as rapid prototyping,^{4–6} steel-making process,^{7,8} microfluidics,^{9–11} and robotics.³ Capillary action provides tremendous application potential for the transport of materials in restricted spaces. For instance, capillary condensation of water allows ink molecules to diffuse from an atomic force microscope tip to the substrate, enabling dip-pen lithography on the nanoscale.⁴ In addition, capillary force plays an important role in liquid transportation in microfluidic chips with a size as small as a coin, which deals with spectrums from chemical synthesis and biological analysis to optics and information technology.^{10,12–14}

Gallium-based eutectic alloys such as EGaIn (75 wt % gallium, 25 wt % indium) and galinstan (68.5 wt % gallium, 21.5 wt % indium, 10 wt % tin) are room-temperature liquid metals bestowed with many excellent properties, such as high electrical and thermal conductivities, low viscosity, high surface tension, and remarkable ability for self-healing, and most importantly, they are much less toxic compared with their counterparts, such as mercury.^{15–17} Hence, such liquid metals have been widely used in the fields of flexible electronics,^{18–22} soft robotics,^{16,23,24} optics,^{25–27} energy harvesting and storage,^{28–30} catalysis, and nanomedicine.^{31–35} In particular, squeezing liquid metal into a

small space or dispersing liquid metal into other porous materials possesses tremendous potentials in making electronic components,^{36–38} thermal interface materials, and microfluidic devices.^{39–41} Recently, electrochemical methods have been used to deposit (or remove) an oxide layer on the surface of an EGaIn droplet to manipulate its surface tension and toggle the droplet in (or out) the capillary, which can be applied to the fabrication of an antenna with a large bandwidth.^{20,42,43} Electrochemically enabled reactive wetting can make liquid metals coat and spread within porous copper.⁴⁴ Moreover, dispersing liquid metals into elastomeric substrates by mechanical mixing can affect the electrical, mechanical, and thermal properties of raw materials^{36–38,45–47} and can even be used to prepare devices with special capabilities, such as self-healing,²¹ and becoming much more conductive upon stretching.³⁶ Nonetheless, all these processes of incorporating liquid metal into other materials require external intervention such as applying electric fields or mechanical stirring, which is inconvenient in forming complex three-dimensional (3D) structures for rapid prototyping.

Preparation of porous materials has the potential to enable gallium-based liquid metals to diffuse spontaneously under the action of capillary forces. Templating and subsequent removal of

Received: November 6, 2019

Accepted: February 10, 2020

Published: February 10, 2020

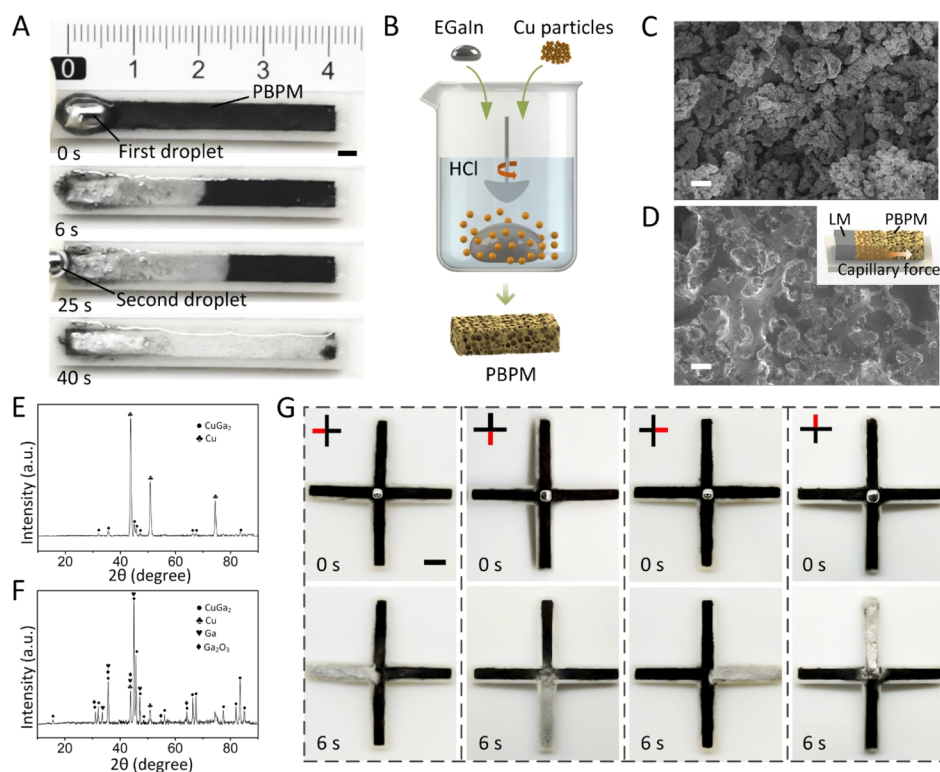


Figure 1. Rapid diffusion of EGaIn liquid metal in the PBPM. (A) Sequential snapshots showing the rapid diffusion of two EGaIn droplets (40 μL each) in the PBPM. The scale bar is 2 mm. (B) Schematic of the process for preparing the PBPM. SEM images of the PBPM (C) before and (D) after the diffusion of EGaIn. The scale bars are 10 μm . XRD spectrums of the PBPM (E) before and (F) after the diffusion of EGaIn. (G) Control of EGaIn diffusion direction using HCl solution; the red squares indicate areas where HCl solution is dropped. The scale bar is 5 mm.

self-assembled colloidal micro/nano particles,⁴⁸ gas foaming,⁴⁹ sugar cubes,⁵⁰ and water droplets⁵¹ are preferred methods to prepare soft porous materials, such as porous polydimethylsiloxane sponges. However, these porous materials have poor wettability for gallium-based liquid metals, which prevents the liquid metals from diffusing into the materials.

In this work, we report a simple yet efficient method to allow liquid metal to spontaneously and rapidly penetrate and diffuse into the particle-based porous materials (PBPMs) using capillary force. In addition to common room-temperature liquid metals, we also investigated the diffusion of other low melting point alloys such as InBiSn (51 wt % indium, 32.5 wt % bismuth, 16.5 wt % tin, melting point of 60.2 $^{\circ}\text{C}$) in the PBPM. Finally, we demonstrated the use of our method for the applications of rapid prototyping and 3D structure printing.

RESULTS AND DISCUSSION

Figure 1A shows the rapid diffusion of EGaIn droplets in the PBPM, which was prepared by mixing copper (Cu) micro-particles (size of $\sim 50 \mu\text{m}$) with EGaIn in condensed hydrochloric acid (HCl) solution (12 M). Specifically, we added 150 mg of Cu particles, 50 μL of EGaIn ($\sim 310 \text{ mg}$), and 3 mL of HCl solution into a clean beaker and stirred the mixture vigorously to allow the Cu particles to be fully wetted by EGaIn, as shown in Figure 1B. The role of HCl solution is to remove the oxide layer formed on the surface of EGaIn during mixing. We observed the generation of hydrogen gas bubbles during the process (see Supporting Information S1). Eventually, the Cu–EGaIn mix lost its fluidity and became granular, and its color changed from silver to dark gray. To prepare the PBPM, we first cleaned the granular product three times with deionized water

and then filled a cuboid channel (40 mm \times 4 mm \times 1 mm) with the granular product ($\sim 400 \text{ mg}$). We also added a few drops of HCl solution into the channel to prevent the oxidation of the PBPM. When we placed a droplet of EGaIn ($\sim 40 \mu\text{L}$) onto one end of the PBPM, despite the large surface tension of EGaIn, we found that the droplet can penetrate swiftly into the PBPM and then rapidly diffuse along the channel. The entire droplet could be fully dispersed within the PBPM in $\sim 6 \text{ s}$, as shown in Figure 1A (also see Movie S1). After adding one additional droplet of EGaIn, the entire PBPM within the channel could be filled with the liquid metal in $\sim 15 \text{ s}$. Interestingly, HCl solution was expelled from the PBPM as EGaIn diffused through the channel (see Figure 1A).

Figure 1C, D, respectively, shows the scanning electron microscopy (SEM) images of the PBPM before and after filling with EGaIn. It can be clearly seen that the PBPM has a porous microstructure, and the pores can be filled with EGaIn because of capillary effect. We believe that the capillary force is the main factor for the rapid penetration and diffusion of liquid metals within the PBPM (see the inset of Figure 1D). When a liquid metal droplet contacts the PBPM, the liquid metal is subjected to a capillary driving pressure P_c from the pores of PBPM, as described by the Young–Laplace equation

$$P_c = \frac{2\gamma \cos \theta}{r} \quad (1)$$

where γ is the surface tension of EGaIn and θ is the contact angle between EGaIn and PBPM. When θ is an acute angle, the liquid metal can enter the capillary under the action of P_c . Assuming the system is in a steady-state flow condition and according to Poiseuille's law expressing the balance between the viscous force

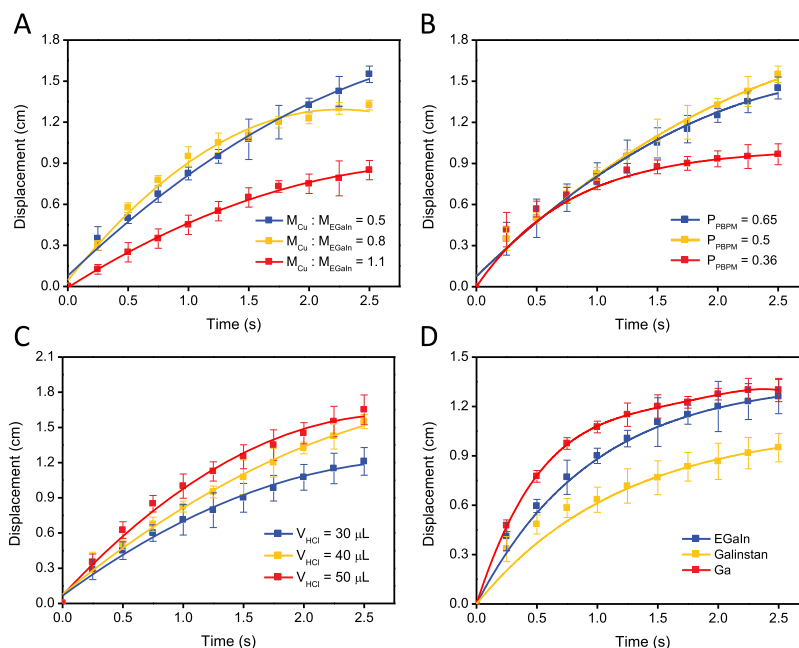


Figure 2. Characterization of the diffusion performance. Diffusion displacement vs time plots for the cases of (A) different $M_{\text{Cu}}/M_{\text{EGaIn}}$ ratios ($P_{\text{PBPM}} = 0.5$, $V_{\text{HCl}} = 40 \mu\text{L}$, EGaIn), (B) different porosities of the PBPM ($M_{\text{Cu}}/M_{\text{EGaIn}} = 0.5$, $V_{\text{HCl}} = 40 \mu\text{L}$, EGaIn), (C) different volumes of the HCl solution ($M_{\text{Cu}}/M_{\text{EGaIn}} = 0.5$, $P_{\text{PBPM}} = 0.5$, EGaIn), and (D) different types of liquid metals ($M_{\text{Cu}}/M_{\text{EGaIn}} = 0.5$, $P_{\text{PBPM}} = 0.5$, $V_{\text{HCl}} = 40 \mu\text{L}$, and the experimental temperature is 40°C).

and capillary force (neglecting inertial and hydrostatic effects), the rate of liquid penetration can be calculated as^{52–54}

$$\frac{\delta l}{\delta t} = \frac{P_c r^2}{8\eta l} \quad (2)$$

where l is the length of EGaIn diffused in the PBPM, t is the time, r is the equivalent pore radius, and η is the viscosity of EGaIn. Combining eqs 1 and 2, the rate and length of diffusion can be calculated as

$$\frac{\delta l}{\delta t} = \frac{r\gamma \cos \theta}{4\eta l} \Rightarrow l = \sqrt{\frac{r\gamma \cos \theta}{2\eta} t} \quad (3)$$

We can see from eq 3 that the length of diffusion (also the rate of liquid penetration) is determined by the wettability of the porous material to EGaIn, which can be quantified by the contact angle θ . We further conducted X-ray diffraction (XRD) analyses to identify the components of the PBPM before and after EGaIn diffusion, as shown in Figure 1E,F, respectively. The spectrum shows that the PBPM mainly contains Cu–Ga alloy and Cu before diffusion, whereas we detected the presence of Ga and its oxide after diffusion. We believe that the formation of CuGa_2 benefits the rapid diffusion of EGaIn in the PBPM by increasing the wettability of the material. To prove our hypothesis, we compared the contact angle of an EGaIn droplet on top of a flat CuGa_2 surface within HCl solution with the case of on a flat Cu surface (see Supporting Information S2). We found that the contact angle between the EGaIn droplet and the CuGa_2 surface is much smaller than that on a Cu surface, indicating that CuGa_2 has much higher wettability to EGaIn.

The HCl solution plays a very important role in the liquid metal's diffusion. A large contact angle of 130° was observed for an EGaIn droplet placed on the surface of the PBPM without HCl solution, and EGaIn cannot diffuse into the PBPM (see Supporting Information S3). This indicates that the HCl solution can improve the wettability of PBPM by removing

the gallium oxide layer on the surface of the liquid metal. EGaIn can amalgamate into the Cu–Ga alloys and therefore, exhibits a higher wettability to CuGa_2 than to HCl solution (see Supporting Information S4). Thus, when EGaIn enters the porous material, HCl solution is expelled from the PBPM during the diffusion process. We found that the threshold concentration of the HCl solution that can enable the diffusion of liquid metal is $\sim 1.3 \text{ M}$ (see Supporting Information S5). Thus, we can harness this property to control the direction of liquid metal diffusion, as shown in Figure 1G. In addition, we also found that a strong base such as sodium hydroxide (NaOH) solution can also be used to remove the oxide layer on the surface of the liquid metal droplet to allow for the diffusion of liquid metal in the PBPM (see Supporting Information S6).

To understand the diffusion of liquid metals under different conditions, we investigated the diffusion velocity as a function of (1) the ratio of Cu to liquid metal in the PBPM, (2) the total mass of the PBPM with the same volume (i.e., the porosity of the PBPM), (3) the amount of HCl solution added to the PBPM, and (4) the types of liquid metals. Figure 2 shows the diffusion displacement versus time under different conditions, in which the slope of the curve represents the velocity of diffusion. We pretreated the PBPM with $40 \mu\text{L}$ of condensed HCl solution (12 M). Figure 2A indicates that the diffusion velocity of liquid metal is slightly enhanced after increasing the mass ratio of Cu to EGaIn ($M_{\text{Cu}}/M_{\text{EGaIn}}$) from 0.5 to 0.8 when making the PBPM; however, the diffusion rate is compromised when further increasing the ratio to 1.1. It is noteworthy that when $M_{\text{Cu}}/M_{\text{EGaIn}}$ is smaller than 0.5, EGaIn cannot be fully consumed in the mixing process, and the product maintains its fluidity; thus, the desired granular product cannot be formed for making the desired PBPM. When $M_{\text{Cu}}/M_{\text{EGaIn}}$ is larger than 0.8, we found that not all Cu particles can be fully covered by EGaIn when making the PBPM. As such, the excess Cu particles hinder the formation of CuGa_2 in the product and therefore, weaken the wettability of the produced PBPM.

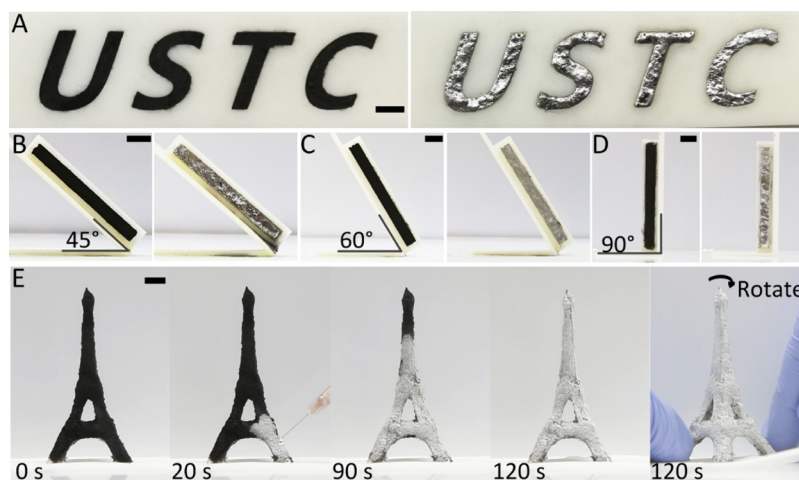


Figure 3. Ability of inducing rapid diffusion of the liquid metal in complex shapes. Diffusion of EGaIn along the PBPM in (A) complex channels, (B–D) channels with different angles of inclination, and (E) 3D structures. The scale bars are 5 mm.

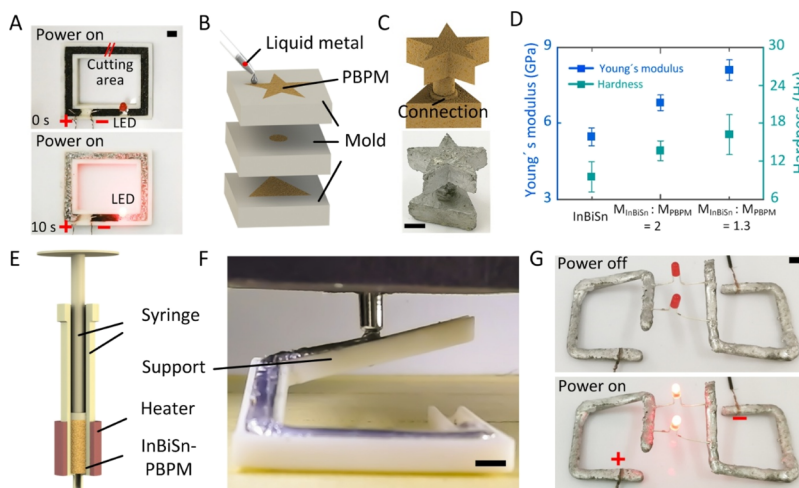


Figure 4. Applications of rapid diffusion of liquid metal. (A) Images showing the rapid diffusion of liquid metal reconnecting a damaged circuit. (B) Schematic showing the manufacture of a pentagonal–cylinder–triangle structure using the rapid prototyping method. (C) Schematic and image of the fabricated pentagonal–cylinder–triangle structure. (D) Comparison of the material mechanical properties before and after mixing InBiSn with the PBPM. (E) Schematic of the 3D printer nozzle. (F) 3D structure printed with the InBiSn–PBPM composite. (G) 3D structure printed with the InBiSn–PBPM composite for the fabrication of 3D circuits. The simple circuit was used for activating a pair of LED lights. The scale bars are 5 mm.

Next, we investigated the effect of porosity of the PBPM (P_{PBPM}) on the diffusion velocity of the liquid metal, as shown in Figure 2B. Because the size of the granular material is unchanged (diameter of $\sim 5 \mu\text{m}$, see Figure 1C), the pore size of the PBPM increases with the increase in porosity. The PBPM samples with different porosities were prepared by filling 150, 200, and 250 mg (fully compacted volume of 29, 40, and 52 mm^3 , respectively) of the Cu–EGaIn granular materials ($M_{\text{Cu}}/M_{\text{EGaIn}} = 0.5$) into a cuboid channel (20 mm \times 4 mm \times 1 mm), which correspond to the PBPM porosities of 0.65, 0.5, and 0.36, respectively. The fully compact volumes of the PBPM were obtained by compressing the granular material with a large pressure of ~ 153 MPa. We can see that decreasing the porosity from 0.65 to 0.5 does not affect the diffusion performance; however, further decreasing the porosity to 0.36 causes a significant reduction in the diffusion velocity (Figure 2B). This can be attributed to the fact that decreasing the porosity of the PBPM can cause a decrease in the equivalent pore radius r and the number of capillaries in a cross-section perpendicular to the direction of diffusion, and according to eq 3, this would lead to a

decrease in the diffusion velocity. We believe that by further reducing the porosity of PBPM, the diffusion velocity will decrease and eventually may prevent the diffusion of liquid metal.

We further discovered that the amount of condensed HCl solution used for pretreating the PBPM also has a great effect on the liquid metal's diffusion velocity, as shown in Figure 2C. In this experiment, we added different volumes of HCl solution ($V_{\text{HCl}} = 30, 40, \text{ and } 50 \mu\text{L}$, respectively) to pretreat the PBPM (200 mg), and we found that a larger volume of HCl solution can lead to a higher diffusion velocity of the liquid metal.

Finally, we investigated the diffusion velocity of different types of liquid metals, as shown in Figure 2D. To ensure that gallium is in a liquid state, we used a heater to maintain the PBPM and liquid metals at $\sim 40^\circ\text{C}$. We found that Ga diffuses the fastest in PBPM, followed by EGaIn and galinstan. We believe the difference in diffusion velocity is caused by the different wettability of liquid metals. The contact angle of gallium on the PBPM is $\sim 25^\circ$, whereas the contact angles for EGaIn and galinstan are ~ 28 and $\sim 42^\circ$, respectively (also see Supporting

Information S3). According to eq 3, a smaller contact angle θ corresponds to a larger diffusion velocity, and this makes gallium diffuse faster among the tested liquid metals.

After examining the parameters affecting the diffusion performance, we further investigated the ability of our method for inducing rapid diffusion of the liquid metal in channels with complex shapes or even in 3D structures. To demonstrate the capability of forming complex patterns, we prepared a “USTC”-shaped channel filled with the PBPM ($M_{\text{Cu}}/M_{\text{EGaIn}} = 0.5$, $P_{\text{PBPM}} = 0.5$, $V_{\text{HCl}} = 40 \mu\text{L}$), as shown in Figure 3A. We selected the ends of each letter as the starting point for diffusing EGaIn liquid metal. EGaIn was able to diffuse evenly and rapidly along the shape of the letters until filling the channels; this process made the black-colored PBPM change to a silver color and become more reflective. In addition, despite the large density of the liquid metal, we found that such a diffusion process within the PBPM can overcome the effect of gravity, and this was demonstrated by diffusing EGaIn along PBPM-filled channels with different tilting angles (45, 60, and 90°), as shown in Figure 3B–D (also see Movie S2). We also used a 3D Eiffel Tower model with the PBPM attached to the surface for demonstrating the diffusion of the liquid metal in complex 3D structures, as shown in Figure 3E. We used a syringe to inject the liquid metal from the bottom of the model, and we observed that EGaIn can diffuse upward and around the 3D model to completely fill the PBPM in ~ 120 s.

Figure 4A illustrates an example of application in which the liquid metal diffusion was used to reconnect circuits that have been mechanically damaged. Although compacted PBPMs have a relatively good electrical conductivity (the electrical conductivity of PBPM made by $M_{\text{Cu}}/M_{\text{EGaIn}} = 0.5$ is $\sim 3.5 \times 10^5 \text{ S m}^{-1}$) and can retain their shapes like rigid wires, circuits constructed from PBPM are vulnerable to tearing, puncture, and other mechanical damage that cause electrical failure. In order to investigate the ability of liquid metal diffusion to heal the PBPM circuits, we buried the positive and ground electrodes of a power supply (voltage of 3 V) and a LED light into a rectangular-shaped channel (Figure 4A), and filled the channel with the PBPM ($M_{\text{Cu}}/M_{\text{EGaIn}} = 0.5$, $P_{\text{PBPM}} = 0.5$, $V_{\text{HCl}} = 40 \mu\text{L}$). Then, we mechanically cut the PBPM to mimic the damage (gap of ~ 1 mm). To fix the circuit, we next dropped EGaIn droplets in an area that was not damaged and far away from the gap. We observed that EGaIn droplets can quickly diffuse into the PBPM and eventually bridge the gap to light up the LED (Figure 4A).

Given that we have demonstrated a rapid and simple method for diffusing liquid metals in porous media, we further established a manufacturing technology for rapid prototyping and additive 3D printing. As shown in a proof-of-concept experiment, we developed a method for rapid casting and connecting separate metallic parts, as illustrated in Figure 4B. Despite the fact that the diffusion of gallium-based liquid metal can increase the mechanical strength of the structure (see Supporting Information S7), the low melting point of gallium limits the application of the printed structure at higher temperatures. To solve this issue, we used the InBiSn (melting point of 60.2 °C) alloy with an acceptable diffusion performance (see Supporting Information S8) in this experiment. Briefly, we first casted the PBPM into three individual molds (in the shapes of a pentagonal star, a cylinder, and a triangle; the molds were preheated to ~ 50 °C), and then, we added the molten InBiSn (~ 80 °C) alloy into the molds to allow it to diffuse through the PBPM structure (Figure 4B). All the added molten InBiSn could diffuse through the molds before solidification since the

temperature difference between the preheated molds and the melting point of InBiSn is relatively small. After casting each layer separately, we next deposited some PBPM on the interface of adjacent layers and added a few drops of molten InBiSn. The InBiSn quickly diffused into the PBPM at the interface and formed a stable and solid connection between each part. Figure 4C shows the pentagonal–cylinder–triangle three-layered structure prepared using this method. Such a method not only has the ability for realizing prototyping but also improves the mechanical properties such as the strength and hardness of the alloy, as shown in Figure 4D.

Upon successful demonstration of rapid prototyping using the InBiSn alloy, we further explored the potential of using our method for 3D circuit printing. In doing so, we designed a fused deposition modeling (FDM) 3D printer with a nozzle consisting a syringe, a propulsion module, and a heater, as shown in Figure 4E. The propulsion module was used to push the syringe and inject the printing materials out of the nozzle. We first loaded the InBiSn–PBPM ($M_{\text{InBiSn}}/M_{\text{PBPM}} = 2$) mix into a syringe as the printing ink and then heated it to ~ 80 °C. We next activated the propulsion module to extrude the melted material onto a substrate. The InBiSn–PBPM composite became a paste at 80 °C without exhibiting a large surface tension like pure liquid metal, and therefore, it could be easily drawn into a line after extrusion instead of forming droplets, as shown in Figure 4F. The printed InBiSn–PBPM composite can quickly solidify to form complex 3D structures with the aid of the 3D motion of the printer (Figure 4F). Structures made from this method are not only easy to manufacture but also provide excellent electrical and mechanical properties for the fabrication of 3D electrical circuits, as shown in Figure 4G. Nonetheless, it is worth noting that the large-scale applications of the current method still possess challenges such as low printing accuracy and the need of hazardous condensed HCl solution; however, we believe these problems can be resolved in our future works by improving the printing equipment and introducing other nonhazardous solutions for removing the oxide layer.

CONCLUSIONS

In summary, we reported a method for the rapid and spontaneous diffusion of liquid metals in PBPMs by harnessing the capillary force. The PBPM was fabricated by first reacting EGaIn liquid metal with Cu microparticles in HCl solution and then filling the granular reaction product in a mold. Such a PBPM has excellent wettability to liquid metals in HCl solution because of the existence of the Ga–Cu alloy and can therefore, enable rapid penetration and diffusion of different types of liquid metals under a capillary force. We further demonstrated that the direction of diffusion can be controlled using HCl solution, and such a diffusion process can overcome the effect of gravity despite the large density of liquid metals. Moreover, by harnessing the advantages of such a process, we presented a rapid prototyping method for fabricating 3D structures via rapid casting and connecting individual parts or by 3D printing. The metal-based PBPM can be used as a guide to assist large-scale liquid metal patterning without weakening the electrical and thermal conductivities of the composite. Therefore, we believe that our study has an extensive application potential in the fabrication of large-area conductive film patterns and in transfer-printing technology for wearable electronics.^{44,55} Despite the fact that the wettability between the liquid metal and the silicon-based elastomer is low, it is possible to conduct surface treatment of the elastomer, such as plasma treating and

depositing a thin layer of metal film, for enhancing the wettability. This may allow for the direct and rapid incorporation of the liquid metal into microfluidic systems to enable the applications in, for instance, forming 3D microelectrodes,⁵⁶ making chemical sensing probes,⁵⁷ and fabricating micro-pumps.⁵¹

EXPERIMENTAL SECTION

Materials. EGaIn, galinstan, and gallium were purchased from Santech Materials Co., Ltd. The low-melting-point alloy InBiSn (melting point of 60.2 °C) was purchased from Yongcheng Hardware Machinery Manufacturing Co., Ltd. (China). HCl solution was purchased from Aladdin (AR, 36–38%, China). Cu microparticles were purchased from Xindun Alloy Co., Ltd. (GR, 50 μm, China). All molds mentioned in this work were printed by a 3D printer (Formlabs Form2). The heater was purchased from Yupus Technology Center (China), and syringes were purchased from Ningbo Yuqiu Instrument Co., Ltd. (China).

Diffusion of Liquid Metal in Inclined Channels and 3D Structures. The PBPM was fixed in the channels using a double-sided tape attached to the bottom of the channel. In the same manner, the double-sided tape was used to fix the Cu–EGaIn granular materials on the surface of the 3D model to form the PBPM, and then we used a syringe to drop EGaIn onto one side of the model.

Mechanical Testing. The Young's modulus of the InBiSn–PBPM mix was obtained by stretching the material using a multifunction material tester (MTS 809, MTS Systems Corporation, USA). The hardness of the composite material was measured using a Vickers durometer (DuraScan 70 GS, EMCO-TEST, Austria) with a force of 0.02 kg.

3D Circuit Printing. The 3D printer is based on the modification of a FDM printer (CR-10, Creality, China), in which we removed the original nozzle and retained the original motion control system. We used the retained motion control system to control the nozzle motion path and the printed patterns. The propulsion module consists of a motor (Leadshine S7HS09), a micro control unit (Arduino Carduino UNO R3), and a linear slide that can push the syringe and inject the printing materials. A voltage of 3 V was applied between the two ends of the 3D structure using a DC power supply (RIGOL DP832) for activating the LED lights.

Videos and Photos. Videos were captured by a DSLR camera (Canon 5D Mark II). SEM images were taken using a Merlin Compact SEM (Zeiss, German) microscope. The XRD data was obtained using an XRD system (X'Pert, Philips, Holland).

ASSOCIATED CONTENT

Supporting Information

The Supporting Information is available free of charge at <https://pubs.acs.org/doi/10.1021/acsami.9b20124>.

Reaction of Cu microparticles and EGaIn in HCl solution; contact angle of EGaIn on flat CuGa₂ and Cu substrates; importance of HCl solution; contact angle of HCl on flat CuGa₂; threshold concentration of HCl solution; diffusion of liquid metal in NaOH solution; influence of gallium diffusion on the mechanical strength of the PBPM; comparison of the diffusion performance of InBiSn and EGaIn (PDF)

Rapid diffusion of EGaIn in PBPM (MP4)

Rapid diffusion of EGaIn in channels with different tilting angles (MP4)

AUTHOR INFORMATION

Corresponding Authors

Xiangpeng Li – Robotics and Microsystems Center, School of Mechanical and Electric Engineering, Soochow University, Suzhou 215000, China; State Key Laboratory of Applied Optics,

Changchun Institute of Optics, Changchun 130033, China; Email: licool@suda.edu.cn

Shi-Yang Tang – School of Mechanical, Materials, Mechatronic and Biomedical Engineering, University of Wollongong, Wollongong 2522, Australia; orcid.org/0000-0002-3079-8880; Email: shiyang@uow.edu.au

Shiwu Zhang – CAS Key Laboratory of Mechanical Behavior and Design of Materials, Department of Precision Machinery and Precision Instrumentation, University of Science and Technology of China, Hefei, Anhui 230027, China; Email: swzhang@ustc.edu.cn

Authors

Jian Shu – CAS Key Laboratory of Mechanical Behavior and Design of Materials, Department of Precision Machinery and Precision Instrumentation, University of Science and Technology of China, Hefei, Anhui 230027, China

Yangming Lu – Robotics and Microsystems Center, School of Mechanical and Electric Engineering, Soochow University, Suzhou 215000, China

Erlong Wang – CAS Key Laboratory of Mechanical Behavior and Design of Materials, Department of Precision Machinery and Precision Instrumentation, University of Science and Technology of China, Hefei, Anhui 230027, China

Sizpeng Zhao – CAS Key Laboratory of Mechanical Behavior and Design of Materials, Department of Precision Machinery and Precision Instrumentation, University of Science and Technology of China, Hefei, Anhui 230027, China

Xiangbo Zhou – CAS Key Laboratory of Mechanical Behavior and Design of Materials, Department of Precision Machinery and Precision Instrumentation, University of Science and Technology of China, Hefei, Anhui 230027, China

Lining Sun – Robotics and Microsystems Center, School of Mechanical and Electric Engineering, Soochow University, Suzhou 215000, China

Weihua Li – School of Mechanical, Materials, Mechatronic and Biomedical Engineering, University of Wollongong, Wollongong 2522, Australia; orcid.org/0000-0002-6190-8421

Complete contact information is available at: <https://pubs.acs.org/doi/10.1021/acsami.9b20124>

Author Contributions

J.S. and Y.L. contributed equally. S.Z., S.-Y.T., and X.L. conceived the idea. J.S., S.Z., and X.Z. carried out most of the experiments. The manuscript was written through contributions of all authors. All authors have given approval to the final version of the manuscript.

Notes

The authors declare no competing financial interest.

ACKNOWLEDGMENTS

We thank Hao Wu., Rongjie Li., Tao Fang, and Zhe Tao from USTC for helpful discussions and assistance in the preparation of experiments. This research has been partially supported by the National Natural Science Foundation of China (nos. 51828503, U1713206, and 61503270). S.-Y.T. is the recipient of the Vice-Chancellor's Postdoctoral Research Fellowship funded by the University of Wollongong. X.L. is supported in part by a grant from the NSFC under grant no. 61873339, a grant from the China Postdoctoral Science Foundation under grant no. 2016M590497, a grant from the National Science

Foundation of Jiangsu Province under grant no. BK20190096, and the State Key Laboratory of Applied Optics.

REFERENCES

- (1) van Honschoten, J. W.; Brunets, N.; Tas, N. R. Capillarity at the Nanoscale. *Chem. Soc. Rev.* **2010**, *39*, 1096–1114.
- (2) Ajayan, P. M.; Iijima, S. Capillarity-Induced Filling of Carbon Nanotubes. *Nature* **1993**, *361*, 333–334.
- (3) Liu, J. L.; Li, S. P. Capillarity-Driven Migration of Small Objects: A Critical Review. *Eur. Phys. J. E: Soft Matter Biol. Phys.* **2019**, *42*, 1.
- (4) Piner, R. D.; Zhu, J.; Xu, F.; Hong, S.; Mirkin, C. A. “Dip-pen” Nanolithography. *Science* **1999**, *283*, 661–663.
- (5) Deladi, S.; Tas, N. R.; Berenschot, J. W.; Krijnen, G. J. M.; de Boer, M. J.; Peter, M.; Elwenspoek, M. C.; Elwenspoek, M. C. Micro-machined Fountain Pen for Atomic Force Microscope-Based Nanopatterning. *Appl. Phys. Lett.* **2004**, *85*, 5361–5363.
- (6) Kim, K.-H.; Moldovan, N.; Espinosa, H. D. A Nanofountain Probe with Sub-100 nm Molecular Writing Resolution. *Small* **2005**, *1*, 632–635.
- (7) Farajzadeh, R.; Andrianov, A.; Krastev, R.; Hirasaki, G. J.; Rossen, W. R. Foam-Oil Interaction in Porous Media: Implications for Foam Assisted Enhanced Oil Recovery. *Adv. Colloid Interface Sci.* **2012**, *183–184*, 1–13.
- (8) Zhang, H.; Nikolov, A.; Wasan, D. Enhanced Oil Recovery (EOR) Using Nanoparticle Dispersions: Underlying Mechanism and Imbibition Experiments. *Energy Fuels* **2014**, *28*, 3002–3009.
- (9) Whitesides, G. M. The Origins and the Future of Microfluidics. *Nature* **2006**, *442*, 368–373.
- (10) Sackmann, E. K.; Fulton, A. L.; Beebe, D. J. The Present and Future Role of Microfluidics in Biomedical Research. *Nature* **2014**, *507*, 181–189.
- (11) Terray, A.; Oakey, J.; Marr, D. W. M. Microfluidic Control Using Colloidal Devices. *Science* **2002**, *296*, 1841–1844.
- (12) Grunze, M. SURFACE SCIENCE: Driven Liquids. *Science* **1999**, *283*, 41–42.
- (13) Baum, P. Laser-Driven Nanoparticle Motion in Liquids. *Science* **2017**, *355*, 458–459.
- (14) Zhang, M.; Wang, L.; Hou, Y.; Shi, W.; Feng, S.; Zheng, Y. Controlled Smart Anisotropic Unidirectional Spreading of Droplet on a Fibrous Surface. *Adv. Mater.* **2015**, *27*, 5057–5062.
- (15) Dickey, M. D. Stretchable and Soft Electronics Using Liquid Metals. *Adv. Mater.* **2017**, *29*, 1606425.
- (16) Shu, J.; Tang, S.-Y.; Feng, Z.; Li, W.; Li, X.; Zhang, S. Unconventional Locomotion of Liquid Metal Droplets Driven by Magnetic Fields. *Soft Matter* **2018**, *14*, 7113–7118.
- (17) Tang, S.-Y.; Khoshmanesh, K.; Sivan, V.; Petersen, P.; O’Mullane, A. P.; Abbott, D.; Mitchell, A.; Kalantar-zadeh, K. Liquid Metal Enabled Pump. *Proc. Natl. Acad. Sci. U.S.A.* **2014**, *111*, 3304–3309.
- (18) Wang, Q.; Yu, Y.; Yang, J.; Liu, J. Fast Fabrication of Flexible Functional Circuits Based on Liquid Metal Dual-trans Printing. *Adv. Mater.* **2015**, *27*, 7109–7116.
- (19) Kim, M.-g.; Alrowais, H.; Pavlidis, S.; Brand, O. Size-Scalable and High-Density Liquid-Metal-Based Soft Electronic Passive Components and Circuits Using Soft Lithography. *Adv. Funct. Mater.* **2017**, *27*, 1604466.
- (20) Khan, M. R.; Trlica, C.; Dickey, M. D. Recapillarity: Electrochemically Controlled Capillary Withdrawal of a Liquid Metal Alloy from Microchannels. *Adv. Funct. Mater.* **2015**, *25*, 671–678.
- (21) Markvicka, E. J.; Bartlett, M. D.; Huang, X.; Majidi, C. An Autonomously Electrically Self-Healing Liquid Metal-Elastomer Composite for Robust Soft-Matter Robotics and Electronics. *Nat. Mater.* **2018**, *17*, 618–624.
- (22) Wissman, J.; Dickey, M. D.; Majidi, C. Field-Controlled Electrical Switch with Liquid Metal. *Adv. Sci.* **2017**, *4*, 1700169.
- (23) Wu, J.; Tang, S.-Y.; Fang, T.; Li, W.; Li, X.; Zhang, S. A Wheeled Robot Driven by a Liquid-Metal Droplet. *Adv. Mater.* **2018**, *30*, 1805039.
- (24) Zhang, J.; Yao, Y.; Sheng, L.; Liu, J. Self-Fueled Biomimetic Liquid Metal Mollusk. *Adv. Mater.* **2015**, *27*, 2648–2655.
- (25) Dickey, M. D.; Chiechi, R. C.; Larsen, R. J.; Weiss, E. A.; Weitz, D. A.; Whitesides, G. M. Eutectic Gallium-Indium (EGaIn): A Liquid Metal Alloy for the Formation of Stable Structures in Microchannels at Room Temperature. *Adv. Funct. Mater.* **2008**, *18*, 1097–1104.
- (26) Wu, P. C.; Zhu, W.; Shen, Z. X.; Chong, P. H. J.; Ser, W.; Tsai, D. P.; Liu, A.-Q. Broadband Wide-Angle Multifunctional Polarization Converter via Liquid-Metal-Based Metasurface. *Adv. Opt. Mater.* **2017**, *5*, 1600938.
- (27) Yu, J. Q.; Yang, Y.; Liu, A. Q.; Chin, L. K.; Zhang, X. M. Microfluidic Droplet Grating for Reconfigurable Optical Diffraction. *Opt. Lett.* **2010**, *35*, 1890–1892.
- (28) Krupenkin, T.; Taylor, J. A. Reverse Electrowetting as a New Approach to High-Power Energy Harvesting. *Nat. Commun.* **2011**, *2*, 448.
- (29) Liu, G.; Kim, J. Y.; Wang, M.; Woo, J.-Y.; Wang, L.; Zou, D.; Lee, J. K. Soft, Highly Elastic, and Discharge-Current-Controllable Eutectic Gallium-Indium Liquid Metal-Air Battery Operated at Room Temperature. *Adv. Energy Mater.* **2018**, *8*, 1703652.
- (30) Wang, S.; Ding, L.; Fan, X.; Jiang, W.; Gong, X. A Liquid Metal-Based Triboelectric Nanogenerator as Stretchable Electronics for Safeguarding and Self-Powered Mechanosensing. *Nano Energy* **2018**, *53*, 863–870.
- (31) Taccardi, N.; Grabau, M.; Debuschewitz, J.; Distaso, M.; Brandl, M.; Hock, R.; Maier, F.; Papp, C.; Erhard, J.; Neiss, C.; Peukert, W.; Görling, A.; Steinrück, H.-P.; Wasserscheid, P. Gallium-Rich Pd-Ga Phases as Supported Liquid Metal Catalysts. *Nat. Chem.* **2017**, *9*, 862–867.
- (32) Esrafilzadeh, D.; Zavabeti, A.; Jalili, R.; Atkin, P.; Choi, J.; Carey, B. J.; Brkljaca, R.; O’Mullane, A. P.; Dickey, M. D.; Officer, D. L.; MacFarlane, D. R.; Daeneke, T.; Kalantar-Zadeh, K. Room Temperature CO₂ Reduction to Solid Carbon Species on Liquid Metals Featuring Atomically Thin Ceria Interfaces. *Nat. Commun.* **2019**, *10*, 865.
- (33) Lu, Y.; Hu, Q. Y.; Lin, Y. L.; Pacardo, D. B.; Wang, C.; Sun, W. J.; Ligler, F. S.; Dickey, M. D.; Gu, Z. Transformable Liquid-Metal Nanomedicine. *Nat. Commun.* **2015**, *6*, 10066.
- (34) Chechetka, S. A.; Yu, Y.; Zhen, X.; Pramanik, M.; Pu, K. Y.; Miyako, E. Light-Driven Liquid Metal Nanotransformers for Biomedical Theranostics. *Nat. Commun.* **2017**, *8*, 15432.
- (35) Yan, J.; Lu, Y.; Chen, G.; Yang, M.; Gu, Z. Advances in Liquid Metals for Biomedical Applications. *Chem. Soc. Rev.* **2018**, *47*, 2518–2533.
- (36) Yun, G. L.; Tang, S.-Y.; Sun, S. S.; Yuan, D.; Zhao, Q. B.; Deng, L.; Yan, S.; Du, H. P.; Dickey, M. D.; Li, W. H. Liquid Metal-Filled Magnetorheological Elastomer with Positive Piezoconductivity. *Nat. Commun.* **2019**, *10*, 1300.
- (37) Wang, J.; Cai, G.; Li, S.; Gao, D.; Xiong, J.; Lee, P. S. Printable Superelastic Conductors with Extreme Stretchability and Robust Cycling Endurance Enabled by Liquid-Metal Particles. *Adv. Mater.* **2018**, *30*, 1706157.
- (38) Cooper, C. B.; Joshipura, I. D.; Parekh, D. P.; Norkett, J.; Mailen, R.; Miller, V. M.; Genzer, J.; Dickey, M. D. Toughening Stretchable Fibers Via Serial Fracturing of a Metallic Core. *Sci. Adv.* **2019**, *5*, No. eaat4600.
- (39) Wang, H.; Yao, Y.; He, Z.; Rao, W.; Hu, L.; Chen, S.; Lin, J.; Gao, J.; Zhang, P.; Sun, X.; Wang, X.; Cui, Y.; Wang, Q.; Dong, S.; Chen, G.; Liu, J. A Highly Stretchable Liquid Metal Polymer as Reversible Transitional Insulator and Conductor. *Adv. Mater.* **2019**, *31*, 1901337.
- (40) Bartlett, M. D.; Kazem, N.; Powell-Palm, M. J.; Huang, X.; Sun, W.; Malen, J. A.; Majidi, C. High Thermal Conductivity in Soft Elastomers with Elongated Liquid Metal Inclusions. *Proc. Natl. Acad. Sci. U.S.A.* **2017**, *114*, 2143–2148.
- (41) Lin, P.; Wei, Z.; Yan, Q.; Xie, J.; Fan, Y.; Wu, M.; Chen, Y.; Cheng, Z. Capillary-Based Microfluidic Fabrication of Liquid Metal Microspheres toward Functional Microelectrodes and Photothermal Medium. *ACS Appl. Mater. Interfaces* **2019**, *11*, 25295–25305.

- (42) Wang, M.; Trlica, C.; Khan, M. R.; Dickey, M. D.; Adams, J. J. A Reconfigurable Liquid Metal Antenna Driven by Electrochemically Controlled Capillarity. *J. Appl. Phys.* **2015**, *117*, 194901.
- (43) Khan, M. R.; Eaker, C. B.; Bowden, E. F.; Dickey, M. D. Giant and Switchable Surface Activity of Liquid Metal Via Surface Oxidation. *Proc. Natl. Acad. Sci. U.S.A.* **2014**, *111*, 14047–14051.
- (44) Ma, J.-L.; Dong, H.-X.; He, Z.-Z. Electrochemically Enabled Manipulation of Gallium-Based Liquid Metals within Porous Copper. *Mater. Horiz.* **2018**, *5*, 675–682.
- (45) Bartlett, M. D.; Fassler, A.; Kazem, N.; Markvicka, E. J.; Mandal, P.; Majidi, C. Stretchable, High-k Dielectric Elastomers through Liquid-Metal Inclusions. *Adv. Mater.* **2016**, *28*, 3726–3731.
- (46) Tang, S.-Y.; Joshipura, I. D.; Lin, Y.; Kalantar-Zadeh, K.; Mitchell, A.; Khoshmanesh, K.; Dickey, M. D. Liquid-Metal Microdroplets Formed Dynamically with Electrical Control of Size and Rate. *Adv. Mater.* **2016**, *28*, 604–609.
- (47) Kazem, N.; Bartlett, M. D.; Majidi, C. Extreme Toughening of Soft Materials with Liquid Metal. *Adv. Mater.* **2018**, *30*, 1706594.
- (48) Li, J.; Zhang, Y. Porous Polymer Films with Size-Tunable Surface Pores. *Chem. Mater.* **2007**, *19*, 2581–2584.
- (49) Jiao, K.; Graham, C. L.; Wolff, J.; Iyer, R. G.; Kohli, P. Modulating Molecular and Nanoparticle Transport in Flexible Polydimethylsiloxane Membranes. *J. Membr. Sci.* **2012**, *401–402*, 25–32.
- (50) Choi, S.-J.; Kwon, T.-H.; Im, H.; Moon, D.-I.; Baek, D. J.; Seol, M.-L.; Duarte, J. P.; Choi, Y.-K. A Polydimethylsiloxane (PDMS) Sponge for the Selective Absorption of Oil from Water. *ACS Appl. Mater. Interfaces* **2011**, *3*, 4552–4556.
- (51) Thurgood, P.; Baratchi, S.; Szydzik, C.; Mitchell, A.; Khoshmanesh, K. Porous PDMS Structures for the Storage and Release of Aqueous Solutions into Fluidic Environments. *Lab Chip* **2017**, *17*, 2517–2527.
- (52) Washburn, E. W. The Dynamics of Capillary Flow. *Phys. Rev.* **1921**, *17*, 273–283.
- (53) Li, K. W.; Zhang, D. F.; Bian, H. Y.; Meng, C.; Yang, Y. N. Criteria for Applying the Lucas-Washburn Law. *Sci. Rep.* **2015**, *5*, 14085.
- (54) Washburn, E. W. Note on a Method of Determining the Distribution of Pore Sizes in a Porous Material. *Proc. Natl. Acad. Sci. U.S.A.* **1921**, *7*, 115–116.
- (55) Khoshmanesh, K.; Tang, S.-Y.; Zhu, J. Y.; Schaefer, S.; Mitchell, A.; Kalantar-Zadeh, K.; Dickey, M. D. Liquid Metal Enabled Microfluidics. *Lab Chip* **2017**, *17*, 974–993.
- (56) Tang, S.-Y.; Zhu, J.; Sivan, V.; Gol, B.; Soffe, R.; Zhang, W.; Mitchell, A.; Khoshmanesh, K. Creation of Liquid Metal 3D Microstructures Using Dielectrophoresis. *Adv. Funct. Mater.* **2015**, *25*, 4445–4452.
- (57) Tang, S.-Y.; Ayan, B.; Nama, N.; Bian, Y.; Lata, J. P.; Guo, X.; Huang, T. J. On-Chip Production of Size-Controllable Liquid Metal Microdroplets Using Acoustic Waves. *Small* **2016**, *12*, 3861–3869.